© 2022. Published by The Company of Biologists Ltd | Journal of Experimental Biology (2022) 225, jeb244466. doi:10.1242/jeb.244466

RESEARCH ARTICLE

Spatial uniformity of action potentials indicates base-to-apex depolarization and repolarization of rainbow trout (*Oncorhynchus mykiss*) ventricle

Ahmed Badr[1,2,*], Minna Hassinen[1] and Matti Vornanen[1]

ABSTRACT

The spatial pattern of electrical activation is crucial for a full understanding of fish heart function. However, it remains unclear whether there is regional variation in action potential (AP) morphologies and underlying ion currents. Because the direction of depolarization and spatial differences in the durations of ventricular APs set limits to potential patterns of ventricular repolarization, we determined AP morphologies, underlying ion currents and ion channel expression in four different ventricular regions (spongy myocardium; and apex, base and middle of the compact myocardium), and correlated them with *in vivo* electrocardiograms (ECGs) in rainbow trout (*Oncorhynchus mykiss*). ECGs recorded from three leads indicated that the depolarization and repolarization of APs propagate from base to apex, and the main depolarization axis of the ventricle is between +90 and +120 deg. AP shape was uniform across the whole ventricle, and little regional differences were found in the density of repolarizing K^+ currents or depolarizing Ca^{2+} and Na^+ currents and the underlying transcripts of ion channels, providing compelling evidence for the suggested excitation pattern. The spatial uniformity of AP durations and base-to-apex propagation of activation with a relatively slow velocity of propagation indicates no special ventricular conduction pathway in the trout ventricle such as the His–Purkinje system of mammalian hearts. The sequence of repolarization is solely determined by activation time without being affected by regional differences in AP duration.

KEY WORDS: Einthoven's triangle, Electrical excitation, Fish heart, Heart axis, Ventricular conduction pathway

INTRODUCTION

Coordinated contraction of the vertebrate heart is determined by the propagation of action potentials (APs) through all cardiomyocytes of the heart. In fish hearts, electrical excitation is initiated in the sinoatrial (SA) pacemaker at the border zone between the sinus venosus and the atrium (Haverinen and Vornanen, 2007; Jensen, 1965; Mackenzie, 1913; Saito, 1969; Saito, 1973; von Skramlik, 1935; Yamauchi and Burnstock, 1968). In the atrial wall, APs propagate quickly along strands of working cardiomyocytes to the atrioventricular (AV) canal, where the velocity of AP propagation slows down, leaving sufficient time to fill the ventricle with blood (Irisawa, 1978; Sedmera et al., 2003). The cycle of electrical excitation of the heart is terminated by a rapidly advancing ventricular AP, which triggers ventricular myocytes to contract almost simultaneously. The ventricles of endothermic hearts have a specialized endocardial conducting system that originates from the branches of the His bundles and ramifies as Purkinje fibers among the working ventricular myocytes (Gourdie et al., 1993; Jensen et al., 2012; Sedmera and Gourdie, 2014; Szabóa et al., 1986). Unlike mammalian and avian hearts, a histologically specialized conduction path has not been unequivocally demonstrated in fish hearts, although some functional studies suggest the existence of an endocardial conduction pathway in the ventricle of zebrafish (*Danio rerio*) and African lungfish (*Protopterus ethiopicus*) (Arbel et al., 1977; Sedmera et al., 2003).

The rhythmic generation of APs and variable rate of AP propagation through the heart are due to the specialized ion current/channel compositions that produce functionally specific APs for each tissue compartment (Chandler et al., 2009; Greener et al., 2009; Greener et al., 2011; Hassinen et al., 2021; Abramochkin et al., 2022). In general, SA and AV nodes, His bundles and Purkinje fibers are histologically identifiable from the adjacent working myocardium with characteristic cellular composition, size and structure, arrangement and relative abundance of connective and muscular tissues, or immunohistochemically by specific molecular markers (Anderson et al., 2009; Boyett, 2009; Jensen et al., 2012; Waller et al., 1993a,b). In mammalian and avian ventricles, APs proceed from the apex to base and from endocardium to epicardium, owing to the His–Purkinje system (Autenrieth et al., 1975). The spread of activation in the fish ventricle is still poorly understood, and it is unclear whether there is a specialized ventricular conduction pathway that quickly transmits APs from the AV canal to the apex of the ventricle. Consistent with the putative existence of a ventricular conduction pathway, apex-to-base depolarization of the zebrafish ventricle has been reported previously (Sedmera et al., 2003; Zhao et al., 2021). However, Jensen et al. (2012) reported that depolarization of the zebrafish ventricle proceeds from base to apex. The reason for the conflicting results is currently unclear. In other studied fish species, including the rainbow trout (*Oncorhynchus mykiss*), the main vector of activation has been reported to go from base to apex (Kibler et al., 2021; Noseda et al., 1962; Vaykshnorayte et al., 2011, 2018).

Because the wave of depolarization (activation) reaches each myocyte at different times, the sequence of ventricular repolarization must be determined by the activation time and the duration of APs at each locus of the ventricular myocardium. Indeed, in mammalian hearts, there are transmural and apicobasal differences in AP duration and underlying ion currents, which affect the repolarization pattern of the ventricles (Bryant et al., 1997;

[1]University of Eastern Finland, Department of Environmental and Biological Sciences, P.O. Box 111, 80101 Joensuu, Finland. [2]Sohag University, Faculty of Science, Department of Zoology, 82524 Sohag, Egypt.

*Author for correspondence (ahmed.osman@uef.fi)

A.B., 0000-0002-9160-9844; M.H., 0000-0002-2653-3708; M.V., 0000-0003-0953-1425

Received 26 April 2022; Accepted 2 August 2022

Journal of Experimental Biology (2022) 225, jeb244466. doi:10.1242/jeb.244466

Cheng et al., 1999; Dean and Lab, 1990; McKinnon and Rosati, 2016; Shipsey et al., 1997; Szentadrassy et al., 2005). It is not known, however, whether there is a similar regional variation in AP morphologies and ion channel/current distribution in the fish ventricle. Because the direction of depolarization (i.e. local activation time) and spatial differences in the durations of ventricular APs set limits for possible patterns of ventricular repolarization, we measured cardiac axis (i.e. direction of depolarization) and regional distribution of AP durations to deduce the pattern of ventricular repolarization and the potential presence of a special ventricular conduction pathway in rainbow trout ventricle. Based on significant histological differences in the ventricular structure of the fish (compact versus spongy myocardium), it was hypothesized that there are spatial heterogeneities of electrical activity between the ventricular regions.

MATERIALS AND METHODS

Animals

Adult rainbow trout [*Oncorhynchus mykiss* (Walbaum 1792), male and female, mean±s.e.m. body mass=24.60±1.45 g, n=41] were obtained from the local fish farm (Kontiolahti, Finland). In the animal facilities of the University of Eastern Finland (Joensuu), the fish were reared in 500-liter aquaria with a computer-controlled temperature regulation system (Computec, Joensuu Finland). The temperature of the aquaria was regulated at 12°C and aerated water (O_2 9.7 mg ml^{-1}) flowed through them. The photoperiod was 12 h:12 h light:dark. The fish were fed five times a week (Ewos, Turku, Finland). Experiments were conducted with the permission of the national animal experimental board in Finland (permissions STH252A and ESAVI/8877/2019).

Isolation of ventricular myocytes

Each rainbow trout was stunned by a blow to the head and killed by pithing. The heart was quickly excised and rinsed in Ca^{2+}-free low-Na^+ solution containing (in mmol l^{-1}): 100 NaCl, 10 KCl, 1.2 KH_2PO_4, 4 $MgSO_4$, 50 taurine, 20 glucose and 10 HEPES [4-(2-hydroxyethyl)-1-piperazineethanesulfonic acid] with pH adjusted to 6.9 at 20°C with KOH. Ventricular myocytes were isolated with enzymatic digestion method described previously in detail (Vornanen, 1997, 1998). First, the heart was perfused for 7 min with Ca^{2+}-free low-Na^+ saline and then enzymatically digested by a 15-min perfusion with the same solution containing collagenase (Type IA; 0.75 mg ml^{-1}), trypsin (Type IX; 0.5 mg ml^{-1}) and fatty-acid-free bovine serum albumin (BSA; 0.75 mg ml^{-1}, all Sigma Aldrich, St Louis, MO, USA). Both solutions were oxygenated with 100% O_2, and the enzyme solution was recycled using a peristaltic pump. After enzymatic digestion, the ventricle was excised and four different regions, the spongy layer and three parts (apex, middle region and base) from the compact layer, were carefully separated as schematically indicated in Fig. 1A. Each part was minced with scissors into small pieces in fresh Ca^{2+}-free low-Na^+ solution and dissociated into single myocytes by agitating them through the opening of a Pasteur pipette. Isolated myocytes were stored at 5°C in Ca^{2+}-free low-Na^+ solution and used within 8 h after isolation.

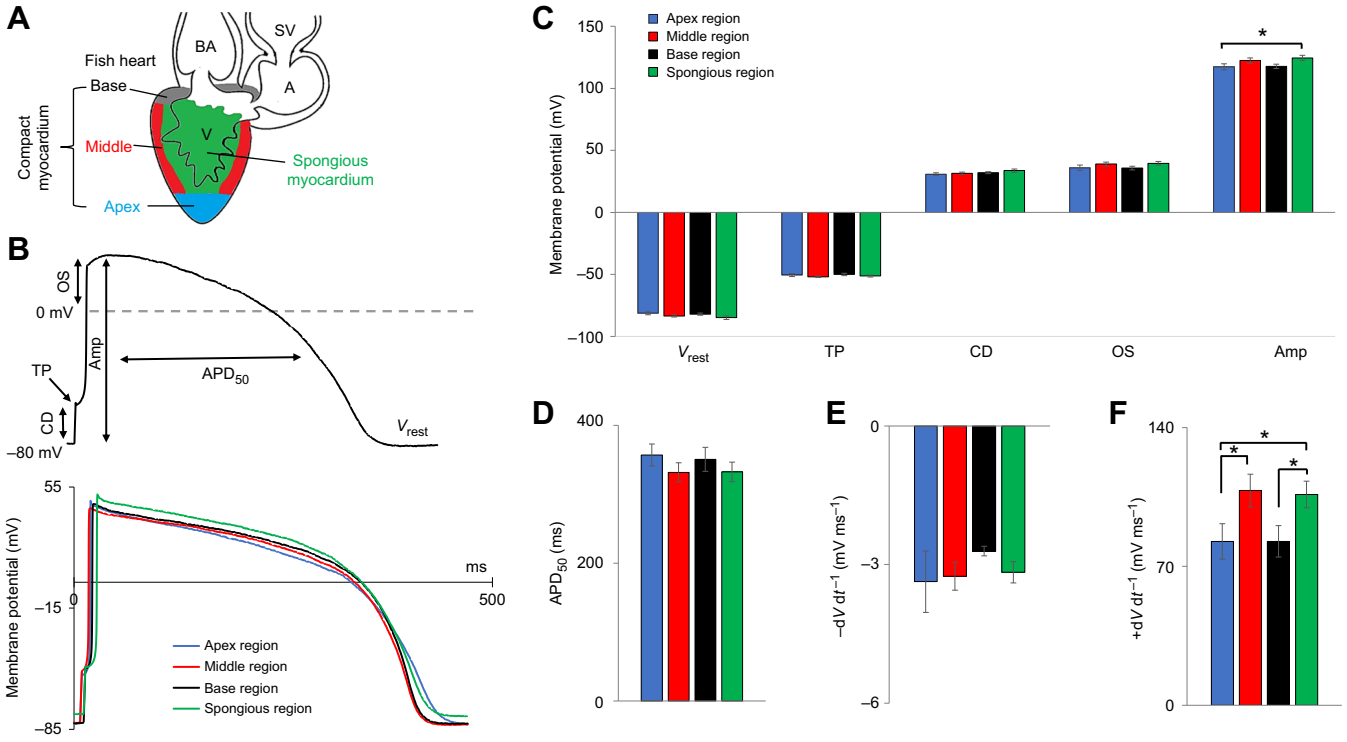

Fig. 1. Ventricular action potentials (APs) waveforms of rainbow trout heart at different regions of the ventricular myocardium (spongy myocardium; and apex, base and middle regions of the compact myocardium) at 12°C. (A) Schematic presentation of myocytes sampling from different locations of the rainbow trout ventricle. (B) Identification of different measured AP parameters (top), and representative registrations of APs from four different ventricular regions (bottom). (C) Mean values of resting membrane potential (V_{rest}), threshold potential for AP initiation (TP), critical depolarization (CD), AP overshoot (OS) and AP amplitude (Amp) for the four different ventricular regions. (D–F) Mean values of AP duration at 50% level of repolarization (APD_{50}; D), maximum rate of repolarization (–dV dt^{-1}; E), and depolarization (+dV dt^{-1}; F). The results are means±s.e.m. of 23–24 myocytes from 10 fish. An asterisk indicates statistically significant differences (*P<0.05; one-way ANOVA) between mean values. BA, bulbus arteriosus; SV, sinus venosus; A, atrium; V, ventricle.

Journal of Experimental Biology (2022) 225, jeb244466. doi:10.1242/jeb.244466

Table 1. Composition of internal (pipette) saline solutions in current clamp and voltage clamp experiments in mmol l^{-1}

	Action potentials	Potassium currents (I_{Kr}, I_{K1})	Sodium current (I_{Na})	Calcium current (I_{CaL})
NaCl			5	
KCl	140	140		
CsCl			130	130
$MgCl_2$	1	1	1	1
TEACl				15
Oxaloacetate				5
MgATP	4	4	5	5
EGTA	5	5	5	5
HEPES	10	10	5	10
cAMP				0.02
pH	7.2 (KOH)	7.2 (KOH)	7.2 (CsOH)	7.2 (CsOH)

Data are from Badr et al. (2017, 2018). TEACl, tetraethyl ammonium chloride; cAMP, cyclic adenosine monophosphate.

Recording of action potentials

Ventricular APs were recorded in the current clamp mode of the whole-cell patch-clamp as described earlier (Badr et al., 2017). The compositions of internal (pipette) and external (bath) solutions are shown in Tables 1 and 2. Patch pipettes were pulled from borosilicate glass (King Precision, Claremont, CA, USA) and when filled with the intracellular saline solution, the mean±s.e.m. electrode resistance was 2.92±0.07 MΩ (n=93). The mean±s.e.m. capacitive size of ventricular myocytes was 31.23±0.80 pF (n=93). The temperature of the external solution was regulated to 12°C using a Peltier device (HCC-100A, Dagan, MN, USA). Myocytes were paced at the frequency of 1 Hz. The digitized data were recorded using Clampex 9.2 software (Axon Instruments, Saratoga, CA, USA) and the recordings were analyzed using the Clampex 10.4 software package. The following AP parameters were analyzed off-line: resting membrane potential (V_{rest}; mV), threshold potential for AP initiation (TP; mV), critical depolarization (CD=TP−V_{rest}; mV), AP overshoot (OS; mV), AP amplitude (Amp; mV), AP duration 50% repolarization level (APD_{50}; ms), the maximum rate of AP upstroke (+dV dt^{-1}; mV ms^{-1}) and the maximum rate of AP repolarization (−dV dt^{-1}; mV ms^{-1}; Fig. 1B).

Recording of ion currents

Ion currents were recorded in the voltage clamp mode of the whole-cell patch-clamp as described earlier in detail (Badr et al., 2017, 2018). Four major ion currents that regulate the shape of ventricular AP in rainbow trout ventricular myocytes were measured: the inward rectifier K^+ current (I_{K1}), the fast component of the delayed rectifier K^+ current (I_{Kr}), the L-type Ca^{2+} current (I_{CaL}) and the Na^+ current (I_{Na}). The compositions of internal and external solutions used for ion current measurements are shown in Tables 1 and 2. When patch pipettes were filled with the intracellular saline solution, the mean±s.e.m. pipette resistance was 3.20±0.04 MΩ (n=218). The mean±s.e.m. capacitive size of ventricular myocytes was 38.86±0.69 pF (n=218). Experimental temperature was 12°C. The size of ion currents is given as current densities (pA pF^{-1}).

Gene expression

Total RNA was extracted from the same regions of the ventricle, where myocytes were isolated for patch-clamp recordings (apex, middle and base of the compact myocardium and the spongy myocardium, n=6) by TRI Reagent Solution (Thermo Fisher Scientific, Vilnius, Lithuania). Transcript levels were determined in triplicate from each sample using Maxima SYBR Green qPCR Master Mix (Thermo Fisher Scientific), specific primers and AriaMx Real-Time PCR System (Agilent Technologies, Santa Clara, CA, USA), as reported previously (Hassinen et al., 2021). The mRNA expression of the studied genes was normalized to the transcript abundance of reference gene *DnaJA2* using the ΔC_t method (Hassinen et al., 2015).

Recording of electrocardiograms

Electrocardiograms (ECGs) were recorded *in vivo* from mildly anesthetized fish (n=11) in the aquarium room (16°C) as previously described (Badr et al., 2016; Vornanen et al., 2014). ECG recordings were analyzed off-line using LabChart 7.1 software (ADInstruments). Fish were anesthetized with neutralized tricaine methanesulfonate (MS-222; 0.3 mg l^{-1}; Sigma Aldrich) for less than 3 min. When the fish was completely immobile and did not

Table 2. Composition of the external (bath) saline solutions in current clamp and voltage clamp experiments in mmol l^{-1}

	Action potentials	I_{Kr} potassium current	I_{K1} potassium current	Sodium current (I_{Na})	L-type Ca current (I_{CaL})
NaCl	150	150	150	20	150
KCl	3	3	3		
CsCl				120	5.4
$MgCl_2$				1	1.2
$MgSO_4$	1.2	1.5	1.5		
NaH_2PO_4	1.2	0.4	0.4		
$CaCl_2$	1.8	2.0	2.0	0.5	1.8
Glucose	10	10	10	10	10
HEPES	10	10	10	10	10
TTX		0.0005	0.0005		0.0005
Nifedipine		0.01	0.01	0.01	
$BaCl_2$		0.2			
E-4031			0.004		
pH (20°C)	7.6 (NaOH)	7.6 (KOH)	7.6 (KOH)	7.6 (CsOH)	7.6 (CsOH)

Data are from Badr et al. (2017, 2018). TTX, tetrodotoxin.

react to handling, it was gently placed on a damp sponge with the abdomen facing up. Aerated water from a 500-liter aquarium (O_2 tension ~9 mg l^{-1}) was continuously administered to the gills through an oral tube. To define the electrical axis of the heart (the major direction of the overall electrical activity of the heart in the frontal plane), three thin steel electrodes (7-strand Teflon-coated wire, 0.23 mm in diameter; A-M Systems, Carlsborg, WA, USA) were inserted under the ventral skin of the fish to mimic the three limb leads of the Einthoven's triangle (Fig. 4A). For lead I (0 deg), the bipolar electrodes were oriented along the horizontal axis of the heart at the same level (slightly above lower edge of the opercula), with the negative (−) electrode on the right and the positive (+) electrode on the left. For leads II and III, the bipolar electrodes were oriented along the longitudinal axis of the heart. In lead II (+60 deg), the negative electrode was positioned at the ventricular base on the right and the positive electrode close to the apex of the heart on the left. In lead III (+120 deg), the negative electrode was positioned at the ventricular base on the left and the positive electrode close to the apex of the heart on the right (Dupre et al., 2005). In all leads, the reference electrode was inserted near the anus.

In ECGs, a wave of depolarization traveling toward the positive electrode displays a positive voltage on the ECG tracing. Thus, in the case of ventricular depolarization (QRS complex), if the R wave is larger than the S wave, then depolarization propagates towards the positive electrode, but if the S wave is larger than the R wave, then depolarization propagates away from the positive electrode. If R and S waves are equal in size, then depolarization spreads perpendicular to the vector of that lead (isoelectric). The electrical axis of the fish ventricle can be obtained as a sector overlap in the circle formed by the vectors of the three leads. It is noteworthy that if the T wave (repolarization of the ventricle) is concordant with the QRS complex, i.e. it has the same polarity as the QRS wave, then repolarization occurs in the opposite direction to depolarization in that lead (Dössel et al., 2021; Janse et al., 2012). If QRS and T waves are discordant, then repolarization occurs in the same direction as depolarization.

Statistics

The results are represented as means±s.e.m. Normality of distribution was tested using Shapiro–Wilk test, and if the data failed the assumption of normality, logarithmic transformations were made. After checking the equality of variances, statistical comparison of mean values of APs, ion currents, mRNA amounts and ECG parameters were performed using one-way ANOVA. Tukey's and LSD (in the case of equal variances) or Dunnett's T3 (unequal variances) *post hoc* tests were used for paired comparisons. Differences were considered statistically significant when $P<0.05$.

RESULTS

Action potentials

APs were measured in enzymatically isolated ventricular myocytes from four different regions (spongy myocardium; and apex, base and middle region of the compact myocardium) (Fig. 1A). APs from the spongious myocardium and different regions of the compact ventricular myocardium had similar shapes (Fig. 1B). V_{rest}, TP, CD, OS, $-dV\,dt^{-1}$ and APD_{50} were not different between the different regions ($P>0.05$) (Fig. 1C–E). Amplitude of the AP was 5.8% higher in the spongiosa compared with the apex ($P<0.05$), and the maximum rate of depolarization ($+dV\,dt^{-1}$) was slightly higher (22.3–23.7%) in the middle region and spongiosa than in the base and apex ($P<0.05$; Fig. 1F).

Outward K^+ currents and transcript expression of K^+ channels

I_{K1} was elicited from the holding potential of −80 mV by voltage ramps from +60 to −120 mV at the frequency of 0.2 Hz using the established voltage protocol (Fig. 2A). There were no differences in I_{K1} density between different regions of the ventricle either for the inward current (IC) or the outward current (OC) (Fig. 2B). The I_{K1} is produced by various Kir2 channels, of which Kir2.4, Kir2.2b and Kir2.1a account for approximately 98% of the I_{K1} in rainbow trout ventricular myocytes (Hassinen et al., 2021). Consistent with the I_{K1} density, there were no differences in the expression of the three major isoforms of I_{K1}-producing Kir2 encoding genes between the different regions of the ventricle (Fig. 2C).

I_{Kr} was elicited from the holding potential of −80 mV using a two-step voltage protocol at the frequency of 0.2 Hz using the established voltage protocol (Fig. 2D). There were no significant differences in I_{Kr} density between different regions of the ventricle (Fig. 2E). The I_{Kr} is produced by various erg encoding genes, of which *KCNH6a* (erg2) alone accounts for approximately 99.7% of the current in rainbow trout ventricle (Hassinen et al., 2021). Consistent with the I_{Kr} density, there were no differences in the expression of the two isoforms of I_{Kr}-producing erg genes (*KCNH6a* and *KCNH2bb*) between the different regions of the ventricle (Fig. 2F).

Inward currents and transcript expression of Ca^{2+} and Na^+ channels

Ca^{2+} current (I_{Ca}) was elicited from the holding potential of −80 mV in the presence of 0.5 µmol l^{-1} TTX, which completely blocks I_{Na} (Fig. 3A). The threshold voltage of I_{Ca} was approximately −30 mV and the peak density of I_{Ca} occurred at 0 mV for all four regions of the trout ventricle suggesting that major part of the charge was carried by L-type Ca^{2+} current (I_{CaL}). There were no statistically significant differences in the peak I_{CaL} density at 0 mV between different regions of the ventricle (Fig. 3B). I_{Ca} of rainbow trout ventricle is produced by a variety of Ca^{2+} channel genes (Hassinen et al., 2021). L-type Ca^{2+} channel *cacna1c* was the major component in all regions except the base, where *cacna1c* and the T-type Ca^{2+} channel *cacna1ga* were equally expressed (Fig. 3C). Of the minor Ca^{2+} components, L-type Ca^{2+} channel *cacna1daa* and T-type Ca^{2+} channel *cacna1ha* were more highly expressed in the base than in other regions of the ventricle ($P<0.05$), whereas no differences were found in T-type Ca^{2+} channel *cacna1hb* between different regions of the ventricle. The combined expression level of all Ca^{2+} channels did not differ between the four tissue regions ($P>0.05$; Fig. 3C).

Na^+ current (I_{Na}) was elicited from the holding potential of −120 mV every 1 s (Fig. 3D). The peak current density was between −30 and −20 mV. There were no statistically significant differences in the peak current density of I_{Na} between different regions of the ventricle (Fig. 3E). I_{Na} is produced by several Na^+ channel α-subunits in the rainbow trout ventricle, of which *SCN4Aba* and *SCN5LAbb* are the dominant isoforms (Hassinen et al., 2021). Consistent with the I_{Na} density, there were no statistically significant differences in the combined expression of the four α-subunit isoforms between different regions of the ventricle ($P>0.05$) (Fig. 3F). However, the expression of *SCN4Abb* was higher in the base than in other regions, and the expression of *SCN5LAba* in the base was lower than that in the apex and spongiosa.

Determination of heart axis

The positions of the bipolar electrodes and the vectors of three ECG leads, and typical recordings from leads I, II and III are shown in Fig. 4A,B. The P wave and QRS complex correspond to atrial and

Journal of Experimental Biology (2022) 225, jeb244466. doi:10.1242/jeb.244466

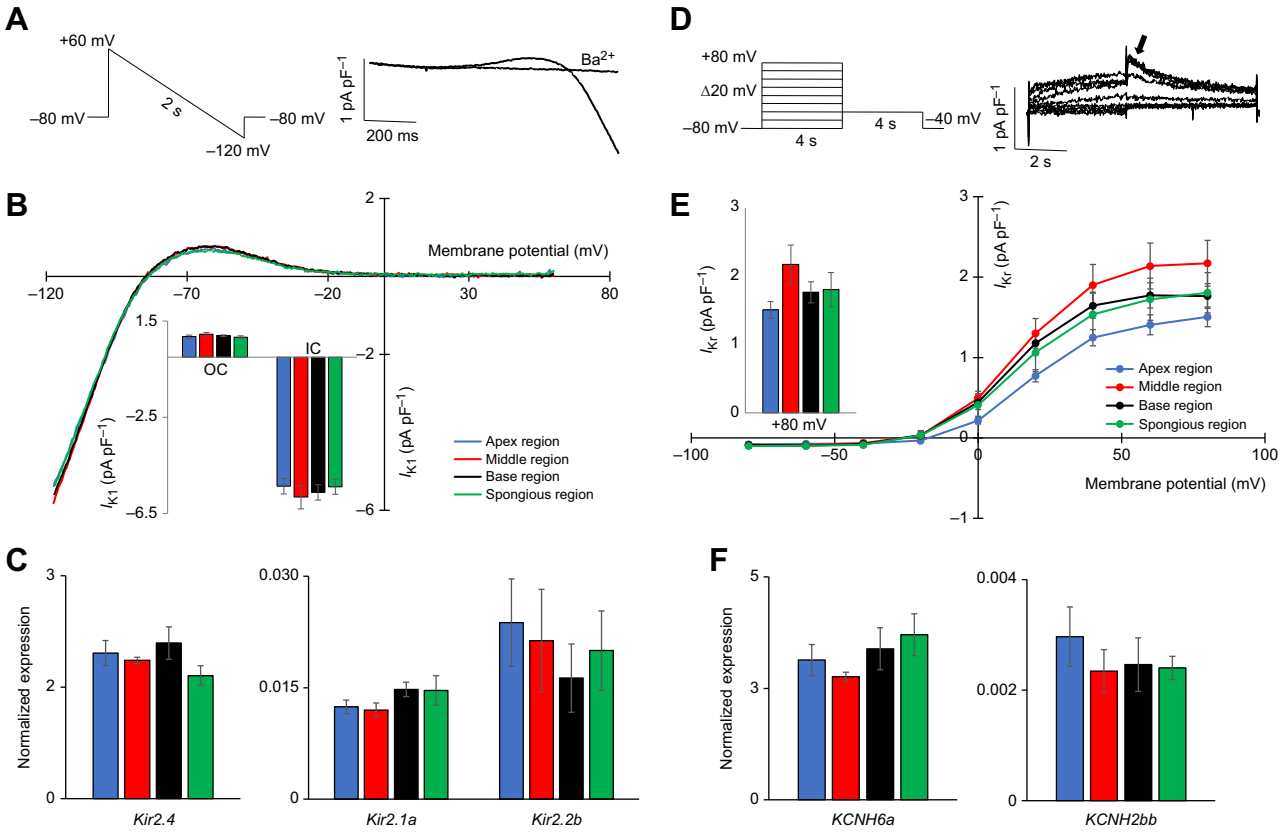

Fig. 2. Inward and delayed rectifier K$^+$ currents in myocytes from different regions of the rainbow trout ventricle at 12°C. (A–C) Inward rectifier K$^+$ current (I_{K1}). (A) Voltage protocol and representative I_{K1} tracings at different membrane potentials. (B) Representative I_{K1} tracings showing the voltage-dependence of I_{K1}. Peak densities of inward (IC) and outward (OC) I_{K1} are shown in the inset. (C) Transcripts of Kir2 inward rectifier K$^+$ channel encoding genes. The results are means±s.e.m. of 11–13 myocytes from four fish for I_{K1} recordings and from six fish for transcript expression. (D–F) Delayed rectifier K$^+$ current (I_{Kr}). (D) Voltage protocol and representative I_{Kr} tracings at different membrane potentials. The arrow indicates the point of measurement (the maximum tail current amplitude). (E) Current–voltage relationship of I_{Kr} from different regions of rainbow trout ventricle. The inset shows the peak tail current densities at +80 mV. (F) Transcript expression of *KCNH2bb* and *KCNH6a* genes. The results are means±s.e.m. of 15–20 myocytes from five fish for I_{Kr} recordings and from six fish for transcript expression.

ventricular depolarization, respectively, whereas the T wave represents the repolarization of the ventricle. The R wave is bigger than the S wave (positive QRS polarity) in leads II (+60 deg) and III (+120 deg) but smaller than the S wave (negative QRS polarity) in lead I (0 deg) (Fig. 4B,C). Furthermore, the amplitude of the R wave is approximately 50% higher in lead III than in leads I and II (P<0.05; Fig. 4E), suggesting that the vector of lead III is closest to the heart axis. Indeed, the overlap of the lead vectors (shaded areas of circles in Fig. 4F) indicates that the cardiac axis is between +90 and +120 deg, i.e. the main axis of ventricular depolarization is from base to apex. The T wave is discordant with the R wave in the three leads, suggesting that repolarization and depolarization of the ventricle in the three leads occur in the same direction (Fig. 4B–D). Given that lead III is almost parallel to the heart axis, the discordant T wave indicates that the main direction of repolarization in rainbow trout ventricle is from base to apex.

Mean duration of the QRS complex (activation) measured from the three EGC leads was 51.5±1.2 ms. As the total length of the trout ventricle was approximately 6 mm, the rate of AP propagation in the ventricular wall was approximately 0.12 m s^{-1}.

DISCUSSION

Analysis of APs, ion currents and transcript expression of ion channel α-subunits show little regional heterogeneity in the molecular and cellular basis of electrical excitation in the rainbow trout ventricle. Measurement of APs and ion currents indicate that electrical excitation is homogeneous at the level of isolated ventricular myocytes. This differs from several observations on mammalian cardiac myocytes, which show large regional differences in the shape of ventricular APs, underlying ion currents and ion channel expression (Antelevitch and Fish, 2001; Gaborit et al., 2007; McKinnon and Rosati, 2016; Schram et al., 2002; Szentadrassy et al., 2005; Watanabe et al., 1983). It might be assumed that the situation would be different if APs were measured from an intact fish ventricle. In multicellular tissue, myocytes are electrically coupled to each other, and electrotonic current flow between myocytes will attenuate, not increase, differences in AP shape (Anyukhovsky et al., 1999; Janse et al., 2012).

The conduction of depolarization and repolarization of the endothermic (mammalian and avian) hearts can be reduced to the consensus view that the major direction of depolarization is from apex to base and that the last activated regions repolarize first because they have the shortest APs. Therefore, the main direction of repolarization is from base to apex and from epicardium to endocardium, although this concept has been questioned (Christian and Scher, 1967; Opthof et al., 2017). This excitation pattern is structurally and functionally based on the rapid conduction pathway of the His–Purkinje system and apicobasal and transmural

Journal of Experimental Biology (2022) 225, jeb244466. doi:10.1242/jeb.244466

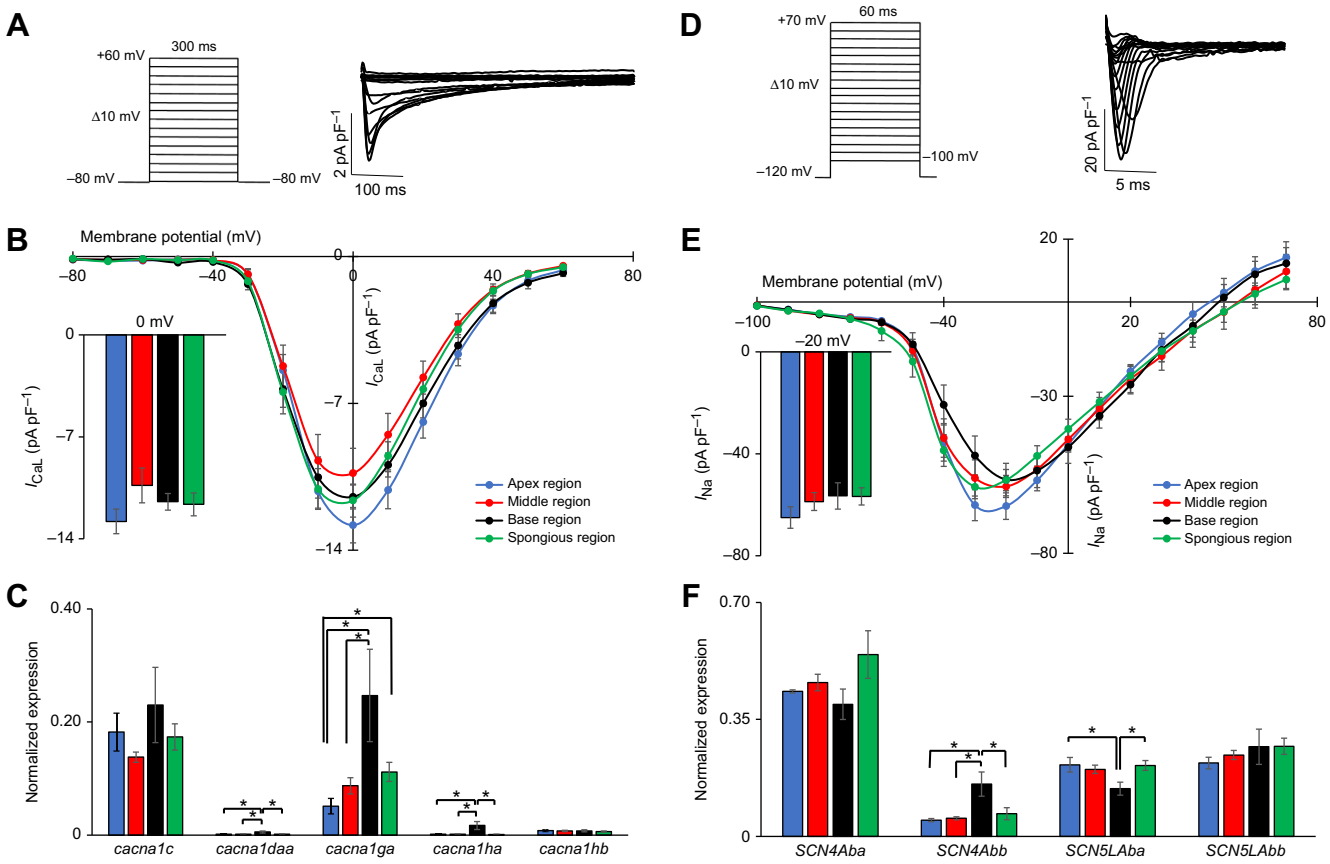

Fig. 3. L-type Ca^{2+} and Na^{+} currents in myocytes from different regions of the rainbow trout ventricle at 12°C. (A–C) L-type Ca^{2+} current (I_{CaL}). (A) Voltage protocol and representative I_{CaL} tracings at different membrane potentials. (B) Mean current–voltage relationship of I_{Ca} in the four different regions of the rainbow trout ventricle. The inset shows the peak current densities at 0 mV. (C) Expression of Ca^{2+} channel transcripts in the four ventricular regions. The results are means±s.e.m. of 13–17 myocytes from four fish for I_{Ca} recordings and from six fish for transcript expression. (D–F) Na^{2+} current (I_{Na}). (D) Voltage protocol and representative I_{Na} tracings at different membrane potentials. (E) Mean current–voltage relationship of I_{Na} in the four different regions of the rainbow trout ventricle. The inset shows the peak I_{Na} densities at –20 mV. (F) Expression of Na^{2+} channel transcripts in the four ventricular regions. The results are means±s.e.m. of 10–12 myocytes from three fishes for I_{Na} recordings and from six fish for transcript expression. An asterisk indicates statistically significant differences (*P<0.05; one-way ANOVA) between means.

differences of AP durations and ion current densities. Owing to the fast-conducting His–Purkinje system, the effect of activation time to repolarization pattern may be small in endothermic hearts (Ramanathan et al., 2006). In contrast, hearts of embryonic endotherms and adult ectotherms seem to lack an anatomically distinct ventricular conduction pathway similar to the His–Purkinje system, and therefore in these hearts activation may occur from base to apex (Jensen et al., 2012). The present ECG recordings indicate that the main cardiac axis is indeed oriented craniocaudally, suggesting that depolarization of the rainbow trout ventricle occurs from base to apex. This is consistent with activation patterns of cod (*Gadus morhua*), pike (*Esox lucius*) and rainbow trout ventricle determined by multielectrode arrays (Azarov et al., 2013; Kibler et al., 2021; Vaykshnorayte et al., 2011, 2022). In these teleost species, the earliest activation occurs in the endocardial surface of the dorsal base near the atrioventricular orifice and spreads from there toward the ventral areas of the base and at the same time to the apex of the ventricle. Optical mapping of activation in the zebrafish heart indicates an activation pattern similar to that of cod, pike and trout (Jensen et al., 2012). However, the results for zebrafish are partly contradictory, as activation has also been shown to propagate from apex to base (Sedmera et al., 2003; Zhao et al., 2021). Two of the zebrafish studies (Jensen et al., 2012; Zhao et al., 2021) used the same voltage-sensitive dye, di-4-ANEPPS, for optical mapping. The fact that a different conclusion was reached using the same recording method suggests that differences in experimental conditions might explain the conflicting results. As the depolarization pattern has only been studied in a few teleost species, it is impossible to make any generalization of the ventricular activation pattern in fish. However, current observations indicate base-to-apex type of activation in most of the species studied.

The direction of ventricular repolarization is dependent on the spatial spread of depolarization (activation time) and AP duration (Janse et al., 2012). The current ECG recordings in rainbow trout reveal that the repolarization proceeds from base to apex. In the three leads, the T wave had an opposite polarity than the R wave, indicating that repolarization proceeded in the same direction as depolarization in these leads. The base-to-apex repolarization is consistent with multielectrode array studies in this species, which showed the earliest repolarization in the ventral base and then in the dorsal base and apex of the ventricle (Kibler et al., 2021). The homogeneity of AP durations throughout the rainbow trout ventricle is consistent with the base-to-apex repolarization pattern. In fact, similarity of AP durations does not allow for apex-to-base repolarization. In rainbow trout ventricle, activation reaches the apex within approximately 52 ms from the first depolarization at the base. During this time, APs of the basal myocytes have already started repolarization, which therefore must proceed towards the

Journal of Experimental Biology (2022) 225, jeb244466. doi:10.1242/jeb.244466

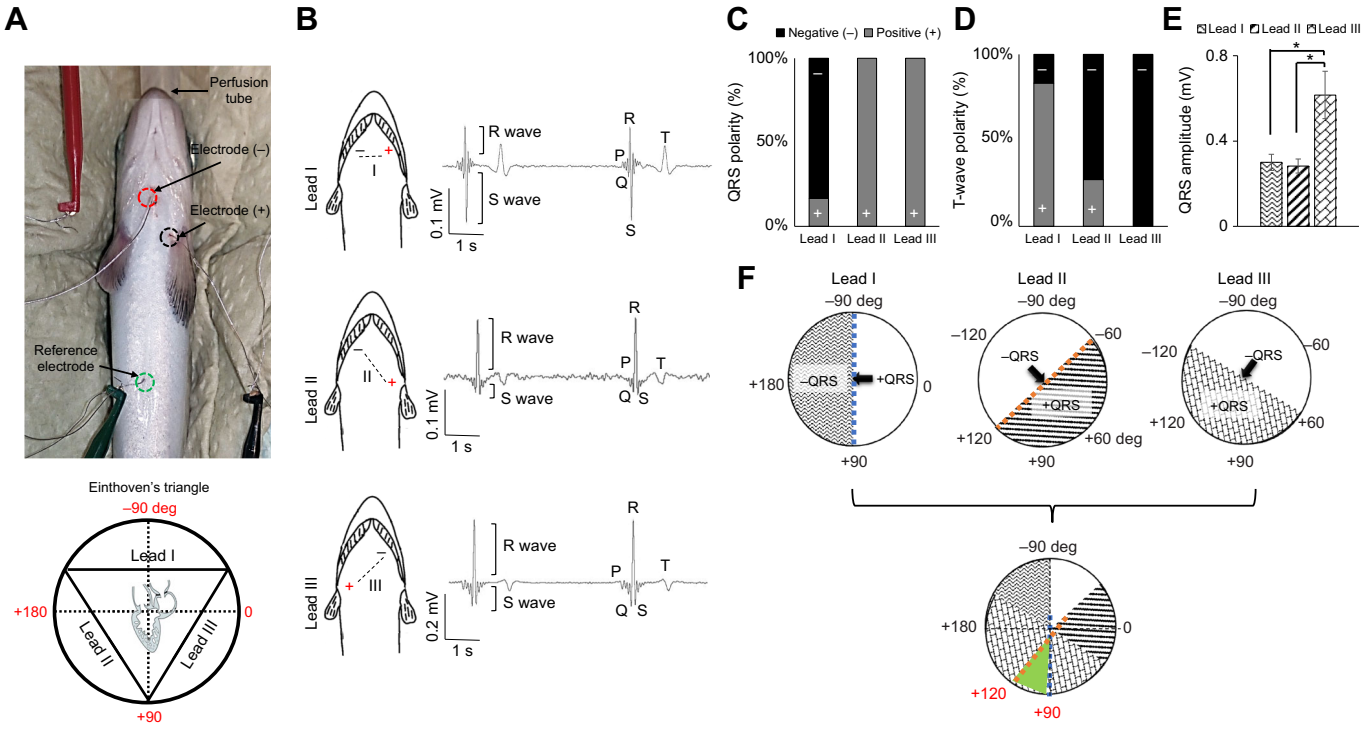

Fig. 4. Determination of the heart axis (the main direction of ventricular depolarization) in rainbow trout by *in vivo* ECG recordings at 16°C. (A) Top: ECG recording set-up in anesthetized rainbow trout lying on a damped sponge and orally perfused for aeration. Bipolar electrodes are inserted at their locations for lead II of the Einthoven's triangle (red and black circles) and the reference electrode inserted near the anus (green circle). Bottom: A diagram shows the directions of the three pairs of electrodes used to construct three leads (I–III) for the Einthoven's triangle (see Materials and Methods). (B) Representative ECG recordings from the three leads. P, atrial depolarization; QRS complex, ventricular depolarization; T, ventricular repolarization; R wave, the positive deflection of QRS complex away from the isoelectric baseline; S wave, the negative deflection of QRS complex away from the isoelectric baseline. (C) Polarity percentage of the QRS complex in the three leads. (D) Polarity percentage of the T wave in the three leads. (E) Amplitude of the QRS complex in the three ECG leads. (F) The main direction of depolarization in the three ECG leads, where the overlapping between them resulted in the rainbow trout heart axis between +90 and +120 deg (green sector). Results are from 11 fish. An asterisk indicates statistically significant differences (*P<0.05; one-way ANOVA) between means.

apex in the same order as depolarization owing to the spatial similarity of AP durations. The spatial homogeneity of AP durations is supported by similar density of the main depolarizing and repolarizing ion currents and similar transcript levels of ion channel α-subunits in different parts of the ventricle. Consistent with this, the ventricle of summer-acclimatized rainbow trout at 18°C shows little difference in activation time and activation–repolarization interval (Vaykshnorayte et al., 2022). Also consistent with the current AP duration data, a multielectrode array study has shown that repolarization time is similar at the base and apex of the rainbow trout ventricle at the sinus rate (Kibler et al., 2021). Notably, when the combined data from the three regions of the compact myocardium were compared with that of the spongy layer, practically no differences were found in APs, ion currents or ion channel expression (Fig. S1). This strongly suggests the absence of transmural heterogeneity of activation and repolarization in the trout ventricle. However, Vaykshnorayte et al. (2022) found transmural and apicobasal differences in activation time and activation–repolarization interval in the ventricle of winter-acclimatized rainbow trout at 3°C, suggesting that the patterns of activation and repolarization may be temperature-dependent. The repolarization pattern of the ventricular epicardium of the pike heart is shown to occur mainly in the apex-to-base direction, although an additional area of early repolarization was found at the posterior ventricular base, i.e. at the site of early depolarization (Vaykshnorayte et al., 2011). Apex-to-base repolarization requires that the durations of APs become shorter from the base of the ventricle towards the apex of the ventricle. Consistent with this, the repolarization time of the apex is slightly shorter in the apex than base of the pike ventricle (Vaykshnorayte et al., 2011). A similar difference in repolarization as between rainbow trout and pike is found also between canine and human hearts: in human ventricles, activation and repolarization proceed in opposite directions, whereas the activation and repolarization follow the same pattern in dog ventricles. Accordingly, in humans, QRS and T waves are concordant, but in the dog, they are discordant (Janse et al., 2012). It seems that the repolarization of the vertebrate ventricle(s) is more variable than depolarization, both within and between species (Opthof et al., 2017). The functional significance of different repolarization patterns remains to be elucidated.

Mammalian ventricles have two types of cardiac myocytes: working ventricular myocytes and conducting Purkinje fibers, the former showing region-specific characteristics of excitability (epicardial, midmyocardial and endocardial myocytes) (Anyukhovsky et al., 1999). In contrast to mammalian ventricles, the rainbow trout ventricle seems to have only working myocardial cells, which are electrophysiologically homogeneous through the ventricular myocardium. This may suggest that specific conduction fibers are absent and therefore electrical excitation propagates along the working myocardial cells throughout the ventricle, which may be an evolutionally old feature and common to the hearts of all ectotherms (Jensen et al., 2012; Boukens et al., 2019). In trout ventricle at 16°C, the rate of AP propagation was approximately 0.12 m s^{-1}. In mammalian Purkinje fibers, the rate of AP

propagation at 37°C is 2 m s^{-1} or slightly higher (Cranefield et al., 1971; Dominguez and Fozzard, 1970), whereas in working ventricular muscle it is approximately 0.6 m s^{-1} (Kelly et al., 2013; McIntyre and Fry, 1997). Using a Q_{10} value of 2.0, the rate of AP propagation in mammalian Purkinje fibers would be approximately 0.47 m s^{-1}, and 0.14 m s^{-1} in working ventricular myocardium at 16°C. The fact that the rate of AP propagation in the trout ventricle is only about one-fourth of the rate of mammalian Purkinje fibers, but similar to the rate of mammalian working myocardium, suggests that conduction does not involve Purkinje fiber-type myocytes. However, if present, the conducting fibers should be electrophysiologically clearly recognizable (e.g. by large I_{Na} and fast $+dV\ dt^{-1}$) from the working cardiac myocytes (Dangman et al., 1982; Makielski et al., 1987). The present study includes patch-clamp recordings from over 300 myocytes from different regions, which is only a tiny fraction of the total myocyte population of the ventricle, and therefore it is possible that not a single conducting fiber was recorded. When searching for a specialized ventricular conducting system, it should be histologically discrete and insulated by a sheath of fibrous tissue from the adjacent working myocardium (Anderson et al., 2009) and characterized by a high density of molecular markers of a fast-conducting tract (e.g. connexins, sodium channels) (Haufe et al., 2005; Kanter et al., 1993). Indeed, Boukens et al. (2019) hypothesized that the electrical conduction delay in the ventricle of ectotherms compared with mammals might be due to the tortuous structure of the spongious myocardium, whereas the compact architecture of mammalian ventricles accelerates electrical conduction independently of the conduction system, as occurs in the mammalian atria.

To our knowledge, this is the first study to look at the expression of AP waveforms, ion currents and ion channels in the fish ventricle. Findings at all organization levels (APs, ion currents, ion channel expression) indicate regional homogeneity of electrical excitation throughout the rainbow trout ventricle. At the organismal level, these findings are consistent with the base-to-apex spread of both depolarization and repolarization, which does not require a specialized ventricular conduction system. From the perspective of ventricular function, this means that at the onset of contraction, the pressure is directed toward the apex of the ventricle, forcing blood to flow through the network of spongious myocardium. Because the basal area relaxes first, blood flows from the apical ventricle towards the base and into the bulbus arteriosus is facilitated by the early increase in the volume of the basal ventricle. Future studies should investigate whether the absence of specialized ventricular conduction system, characterized by high I_{Na} density and fast AP upstroke velocity, sets the upper limit to the heart rate of fish at critically high temperatures (Vornanen, 2020).

Acknowledgements
We thank Anita Kervinen for taking care of fish and preparing solutions for the patch-clamp experiments.

Competing interests
The authors declare no competing or financial interests.

Author contributions
Conceptualization: A.B., M.H., M.V.; Methodology: A.B., M.H.; Formal analysis: A.B., M.H.; Investigation: A.B., M.H.; Writing - original draft: A.B., M.H., M.V.; Writing - review & editing: A.B., M.H., M.V.; Visualization: A.B.; Supervision: M.V.; Project administration: M.V.; Funding acquisition: M.V.

Funding
The present study was supported by the Academy of Finland (project 15051 to M.V.).

References
Abramochkin, D. V., Filatova, T. S., Pustovit, K. B., Voronina, Y. A., Kuzmin, V. S. and Vornanen, M. (2022). Ionic currents underlying different patterns of electrical activity in working cardiac myocytes of mammals and non-mammalian vertebrates. *Comp. Biochem. Physiol. Part A* **268**, 111204. doi:10.1016/j.cbpa.2022.111204

Anderson, R. H., Yanni, J., Boyett, M. R., Chandler, N. J. and Dobrzynski, H. (2009). The anatomy of the cardiac conduction system. *Clin. Anat.* **22**, 99-113. doi:10.1002/ca.20700

Antelevitch, C. and Fish, J. (2001). Electrical heterogeneity within the ventricular wall. *Basic Res. Cardiol.* **96**, 517-527. doi:10.1007/s003950170002

Anyukhovsky, E. P., Sosunov, E. A., Gainullin, R. Z. and Rosen, M. R. (1999). The controversial M cell. *J. Cardiovasc. Electrophysiol.* **10**, 244-260. doi:10.1111/j.1540-8167.1999.tb00667.x

Arbel, E. R., Liberthson, R., Langendorf, R., Pick, A., Lev, M. and Fishman, A. P. (1977). Electrophysiological and anatomical observations on the heart of the African lungfish. *Am. J. Physiol.* **232**, H24-H34. doi:10.1152/ajpheart.1977.232.1.H24

Autenrieth, G., Surawicz, B. and Kuo, C. S. (1975). Sequence of repolarization on the ventricular surface in the dog. *Am. Heart J.* **89**, 463-469. doi:10.1016/0002-8703(75)90152-0

Azarov, J. E., Kibler, N. A., Vaykshnorayte, M. A., Tsvetkova, A. S., Kharin, S. N., Vityazev, V. A. and Shmakov, D. N. (2013). Effect of heart electric stimulation on repolarization of ventricular myocardium of fish and amphibians. *J. Evol. Biochem. Physiol.* **49**, 165-174. doi:10.1134/S0022093013020059

Badr, A., El-Sayed, M. F. and Vornanen, M. (2016). Effects of seasonal acclimatization on temperature-dependence of cardiac excitability in the roach, *Rutilus rutilus*. *J. Exp. Biol.* **219**, 1495-1504. doi:10.1242/jeb.138347

Badr, A., Hassinen, M., El-Sayed, M. F. and Vornanen, M. (2017). Effects of seasonal acclimatization on action potentials and sarcolemmal K^+ currents in roach (*Rutilus rutilus*) cardiac myocytes. *Comp. Biochem. Physiol. A* **205**, 15-27. doi:10.1016/j.cbpa.2016.12.017

Badr, A., Korajoki, H., Abu-Amra, E.-S., El-Sayed, M. F. and Vornanen, M. (2018). Effects of seasonal acclimatization on thermal tolerance of inward currents in roach (*Rutilus rutilus*) cardiac myocytes. *J. Comp. Physiol. B* **188**, 255-269. doi:10.1007/s00360-017-1126-1

Boukens, B. J. D., Kristensen, D. L., Filogonio, R., Carreira, L. B. T., Sartori, M. R., Abe, A. S., Currie, S., Joyce, W., Conner, J., Opthof, T. et al. (2019). The electrocardiogram of vertebrates: evolutionary changes from ectothermy to endothermy. *Prog. Biophys. Mol. Biol.* **144**, 16-29. doi:10.1016/j.pbiomolbio.2018.08.005

Boyett, M. R. (2009). 'And the beat goes on' The cardiac conduction system: the wiring system of the heart. *Exp. Physiol.* **94**, 1035-1049. doi:10.1113/expphysiol.2009.046920

Bryant, S. M., Shipsey, S. J. and Hart, G. (1997). Regional differences in electrical and mechanical properties of myocytes from guinea-pig hearts with mild left ventricular hypertrophy. *Cardiovasc. Res.* **35**, 315-323. doi:10.1016/S0008-6363(97)00111-9

Chandler, N. J., Greener, I. D., Tellez, J. O., Inada, S., Musa, H., Molenaar, P., Difrancesco, D., Baruscotti, M., Longhi, R., Anderson, R. H. et al. (2009). Molecular architecture of the human sinus node: insights into the function of the cardiac pacemaker. *Circulation* **119**, 1562-1575. doi:10.1161/CIRCULATIONAHA.108.804369

Cheng, J., Kamiya, K., Liu, W., Tsuji, Y., Toyama, J. and Kodama, I. (1999). Heterogeneous distribution of the two components of delayed rectifier K current: a potential mechanism of the proarrhythmic effects of methanesulfonanilideclass III agents. *Cardiovasc. Res.* **43**, 135-147. doi:10.1016/S0008-6363(99)00061-9

Christian, E. and Scher, A. M. (1967). The effect of ventricular depolarization on the sequence of ventricular repolarization. *Am. Heart J.* **74**, 530-535. doi:10.1016/0002-8703(67)90012-9

Cranefield, P. F., Klein, H. O. and Hoffman, B. F. (1971). Conduction of the cardiac impulse: I. Delay, block, and one-way block in depressed Purkinje fibers. *Circ. Res.* **28**, 199-219. doi:10.1161/01.RES.28.2.199

Dangman, K. H., Danilo, P., , Jr, Hordof, A. J., Mary-Rabine, L., Reder, R. F. and Rosen, M. R. (1982). Electrophysiologic characteristics of human ventricular and Purkinje fibers. *Circulation* **65**, 362-368. doi:10.1161/01.CIR.65.2.362

Dean, J. W. and Lab, M. J. (1990). Regional changes in ventricular excitability during load manipulation of the *in situ* pig heart. *J. Physiol.* **429**, 387-400. doi:10.1113/jphysiol.1990.sp018263

Dominguez, G. and Fozzard, H. A. (1970). Influence of extracellular K^+ concentration on cable properties and excitability of sheep cardiac Purkinje fibers. *Circ. Res.* **26**, 565-574. doi:10.1161/01.RES.26.5.565

Dössel, O., Luongo, G., Nagel, C. and Loewe, A. (2021). Computer modeling of the heart for ECG interpretation—a review. *Hearts* **2**, 350-368. doi:10.3390/hearts2030028

Dupre, A., Vincent, S. and Iaizzo, P. A. (2005). Basic ECG theory, recordings, and interpretation. In *Handbook of Cardiac Anatomy, Physiology, and Devices* (ed. P. A. Iaizzo), pp. 191-201. Springer.

Gaborit, N., Le Bouter, S., Szuts, V., Varro, A., Escande, D., Nattel, S. and Demolombe, S. (2007). Regional and tissue specific transcript signatures of ion

channel genes in the non-diseased human heart. *J. Physiol.* **582**, 675-693. doi:10.1113/jphysiol.2006.126714

Gourdie, R. G., Green, C. R., Severs, N. J., Anderson, R. H. and Thompson, R. P. (1993). Evidence for a distinct gap-junctional phenotype in ventricular conduction tissues of the developing and mature avian heart. *Circ. Res.* **72**, 278-289. doi:10.1161/01.RES.72.2.278

Greener, I. D., Tellez, J. O., Dobrzynski, H., Yamamoto, M., Graham, G. M., Billeter, R. and Boyett, M. R. (2009). Ion channel transcript expression at the rabbit atrioventricular conduction axis. *Circ. Arrhythm. Electrophysiol.* **2**, 305-315. doi:10.1161/CIRCEP.108.803569

Greener, I. D., Monfredi, O., Inada, S., Chandler, N. J., Tellez, J. O., Atkinson, A., Taube, M.-A., Billeter, R., Anderson, R. H., Efimov, I. R. et al. (2011). Molecular architecture of the human specialised atrioventricular conduction axis. *J. Mol. Cell. Cardiol.* **50**, 642-651. doi:10.1016/j.yjmcc.2010.12.017

Hassinen, M., Haverinen, J., Hardy, M. E., Shiels, H. A. and Vornanen, M. (2015). Inward rectifier potassium current (I_{K1}) and Kir2 composition of the zebrafish (*Danio rerio*) heart. *Pflüg. Arch.* **467**, 2437-2446. doi:10.1007/s00424-015-1710-8

Hassinen, M., Dzumaniiazova, I., Abramochkin, D. V. and Vornanen, M. (2021). Ionic basis of atrioventricular conduction: ion channel expression and sarcolemmal ion currents of the atrioventricular canal of the rainbow trout (*Oncorhynchus mykiss*) heart. *J. Comp. Physiol. B* **191**, 327-346. doi:10.1007/s00360-021-01344-2

Haufe, V., Cordeiro, J. M., Zimmer, T., Wu, Y. S., Schiccitano, S., Benndorf, K. and Dumaine, R. (2005). Contribution of neuronal sodium channels to the cardiac fast sodium current I_{Na} is greater in dog heart Purkinje fibers than in ventricles. *Cardiovasc. Res.* **65**, 117-127. doi:10.1016/j.cardiores.2004.08.017

Haverinen, J. and Vornanen, M. (2007). Temperature acclimation modifies sinoatrial pacemaker mechanism of the rainbow trout heart. *Am. J. Physiol.* **292**, R1023-R1032. doi:10.1152/ajpregu.00432.2006

Irisawa, H. (1978). Comparative physiology of the cardiac pacemaker mechanism. *Physiol. Rev.* **58**, 461-498. doi:10.1152/physrev.1978.58.2.461

Janse, M. J., Coronel, R., Opthof, T., Sosunov, E. A., Anyukhovsky, E. P. and Rosen, M. R. (2012). Repolarization gradients in the intact heart: transmural or apico-basal? *Prog. Biophys. Mol. Biol.* **109**, 6-15. doi:10.1016/j.pbiomolbio.2012.03.001

Jensen, D. (1965). The aneural heart of the hagfish. *Ann. NY Acad. Sci.* **127**, 443-458. doi:10.1111/j.1749-6632.1965.tb49418.x

Jensen, B., Boukens, B. J. D., Postma, A. V., Gunst, Q. D., van den Hoff, M. J., Moorman, A. F. M., Wang, T. and Christoffels, V. M. (2012). Identifying the evolutionary building blocks of the cardiac conduction system. *PLoS ONE* **7**, e44231. doi:10.1371/journal.pone.0044231

Kanter, H. L., Laing, J. G., Beau, S. L., Beyer, E. C. and Saffitz, J. E. (1993). Distinct patterns of connexin expression in canine Purkinje fibers and ventricular muscle. *Circ. Res.* **72**, 1124-1131. doi:10.1161/01.RES.72.5.1124

Kelly, A., Ghouri, I. A., Kemi, O. J., Bishop, M. J., Bernus, O., Fenton, F. H., Myles, R. C., Burton, F. L. and Smith, G. L. (2013). Subepicardial action potential characteristics are a function of depth and activation sequence in isolated rabbit hearts. *Circ. Arrhythm. Electrophysiol.* **6**, 809-817. doi:10.1161/CIRCEP.113.000334

Kibler, N. A., Nuzhny, V. P., Kharin, S. N. and Shmakov, D. N. (2021). Effect of atrial artificial electrical stimulation on depolarization and repolarization and hemodynamics of the heart ventricle in rainbow trout Oncorhynchus mykiss. *Fish Physiol. Biochem.* **47**, 1329-1339. doi:10.1007/s10695-021-00983-0

Mackenzie, I. (1913). The excitatory and connecting muscular system of the heart. *Transcripts of the 17th International Congress of Medicine*, Section 3, pp. 121-150.

Makielski, J. C., Sheets, M. F., Hanck, D. A., January, C. T. and Fozzard, H. A. (1987). Sodium current in voltage clamped internally perfused canine cardiac Purkinje cells. *Biophys. J.* **52**, 1-11. doi:10.1016/S0006-3495(87)83182-X

McIntyre, H. and Fry, C. H. (1997). Abnormal action potential conduction in isolated human hypertrophied left ventricular myocardium. *J. Cardiovasc. Electrophysiol.* **8**, 887-894. doi:10.1111/j.1540-8167.1997.tb00850.x

McKinnon, D. and Rosati, B. (2016). Transmural gradients in ion channel and auxiliary subunit expression. *Prog. Biophys. Mol. Biol.* **122**, 165-186. doi:10.1016/j.pbiomolbio.2016.09.012

Noseda, V., Chiesa, F. and Marchetti, R. (1962). Intracardiac electrocardiography in fishes. *Experienta* **18**, 380-381. doi:10.1007/BF02172263

Opthof, T., Remme, C. A., Jorge, E., Noriega, F., Wiegerinck, R. F., Tasiam, A., Beekman, L., Alvarez-Garcia, J., Munoz-Guijosa, C. and Coronel, R. (2017). Cardiac activation–repolarization patterns and ion channel expression mapping in intact isolated normal human hearts. *Heart Rhythm* **14**, 265-272. doi:10.1016/j.hrthm.2016.10.010

Ramanathan, C., Jia, P., Ghanem, J., Ryu, K. and Rudy, Y. (2006). Activation and repolarization of the normal human heart under complete physiological conditions. *Proc. Natl. Acad. Sci. USA* **103**, 6309-6314. doi:10.1073/pnas.0601533103

Saito, T. (1969). Electrophysiological studies on the pacemaker of several fish hearts. *Zool. Mag.* **78**, 291-296.

Saito, T. (1973). Effects of vagal stimulation on the pacemaker action potentials of carp heart. *Comp. Biochem. Physiol. A* **44**, 191-199. doi:10.1016/0300-9629(73)90381-2

Schram, G., Pourrier, M., Melnyk, P. and Nattel, S. (2002). Differential distribution of cardiac ion channel expression as a basis for regional specialization in electrical function. *Circ. Res.* **90**, 939-950. doi:10.1161/01.RES.0000018627.89528.6F

Sedmera, D. and Gourdie, R. G. (2014). Why do we have Purkinje fibers deep in our heart? *Physiol. Res.* **63** Suppl. 1, S9-S18. doi:10.33549/physiolres.932686

Sedmera, D., Reckova, M., deAlmeida, A., Sedmerova, M., Biermann, M., Volejnik, J., Sarre, A., Raddatz, E., McCarthy, R. A., Gourdie, R. G. et al. (2003). Functional and morphological evidence for a ventricular conduction system in zebrafish and *Xenopus* hearts. *Am. J. Physiol.* **284**, H1152-H1160. doi:10.1152/ajpheart.00870.2002

Shipsey, S. J., Bryant, S. M. and Hart, G. (1997). Effects of hypertrophy on regional action potential characteristics in the rat left ventricle: a cellular basis for T-wave inversion? *Circulation* **96**, 2061-2068. doi:10.1161/01.CIR.96.6.2061

Szabóa, E., Virágh, S. and Challice, C. E. (1986). The structure of the atrioventricular conducting system in the avian heart. *Anat. Rec.* **215**, 1-9. doi:10.1002/ar.1092150102

Szentadrassy, N., Banyasz, T., Biro, T., Szabo, G. Y., Toth, B. I., Magyar, J., Lazar, J., Varro, A., Kovacs, L. and Nanasi, P. P. (2005). Apico–basal inhomogeneity in distribution of ion channels in canine and human ventricular myocardium. *Cardiovasc. Res.* **65**, 851-860. doi:10.1016/j.cardiores.2004.11.022

Vaykshnorayte, M. A., Azarov, J. E., Tsvetkova, A. S., Vityazev, V. A., Ovechkin, A. O. and Shmakov, D. N. (2011). The contribution of ventricular apicobasal and transmural repolarization patterns to the development of the T wave body surface potentials in frogs (*Rana temporaria*) and pike (*Esox lucius*). *Comp. Biochem. Physiol. A* **159**, 39-45. doi:10.1016/j.cbpa.2011.01.016

Vaykshnorayte, M. A., Vityazev, V. A. and Azarov, Y. E. (2018). The sequence of activation of the ventricular myocardium of the Atlantic cod (*Gadus morhua marisalbi*). *Proc. Komi Sci. Cent.* **4**, 431-435.

Vaykshnorayte, M. A., Vityazev, V. A. and Azarov, J. E. (2022). Seasonal changes of electrophysiological heterogeneities in the rainbow trout ventricular myocardium. *Curr. Res. Physiol.* **5**, 93-98. doi:10.1016/j.crphys.2022.02.001

von Skramlik, E. (1935). Über den Kreislauf bei den Fischen. *Ergeb. Biol.* **11**, 1-130. doi:10.1007/978-3-642-91057-9_1

Vornanen, M. (1997). Sarcolemmal Ca influx through L-type Ca channels in ventricular myocytes of a teleost fish. *Am. J. Physiol.* **272**, R1432-R1440. doi:10.1152/ajpregu.1997.272.5.R1432

Vornanen, M. (1998). L-type Ca current in fish cardiac myocytes: effects of thermal acclimation and β-adrenergic stimulation. *J. Exp. Biol.* **201**, 533-547. doi:10.1242/jeb.201.4.533

Vornanen, M. (2020). Feeling the heat: source-sink mismatch as a mechanism underlying the failure of thermal tolerance. *J. Exp. Biol.* **223**, jeb225680. doi:10.1242/jeb.225680

Vornanen, M., Haverinen, J. and Egginton, S. (2014). Acute heat tolerance of cardiac excitation in the brown trout (*Salmo trutta fario*). *J. Exp. Biol.* **217**, 299-309. doi:10.1242/jeb.091272

Waller, B. F., Gering, L. E., Slack, J. D. and Branyas, N. A. (1993a). Anatomy, histology, and pathology of the cardiac conduction system: Part I. *Clin. Cardiol.* **16**, 249-252. doi:10.1002/clc.4960160316

Waller, B. F., Gering, L. E., Branyas, N. A. and Slack, J. D. (1993b). Anatomy, histology, and pathology of the cardiac conduction system: Part II. *Clin. Cardiol.* **16**, 347-352. doi:10.1002/clc.4960160410

Watanabe, T., Delbridge, L. M., Bustamante, J. O. and McDonald, T. F. (1983). Heterogeneity of the action potential in isolated rat ventricular myocytes and tissue. *Circ. Res.* **52**, 280-290. doi:10.1161/01.RES.52.3.280

Yamauchi, A. and Burnstock, G. (1968). An electron microscopic study on the innervation of the trout heart. *J. Comp. Neurol.* **132**, 567-588. doi:10.1002/cne.901320406

Zhao, Y., James, N. A., Beshay, A. R., Chang, E. E., Lin, A., Bashar, F., Wassily, A., Nguyen, B. and Nguyen, T. P. (2021). Adult zebrafish ventricular electrical gradients as tissue mechanisms of ECG patterns under baseline vs. oxidative stress. *Cardiovasc. Res.* **117**, 1891-1907. doi:10.1093/cvr/cvaa238

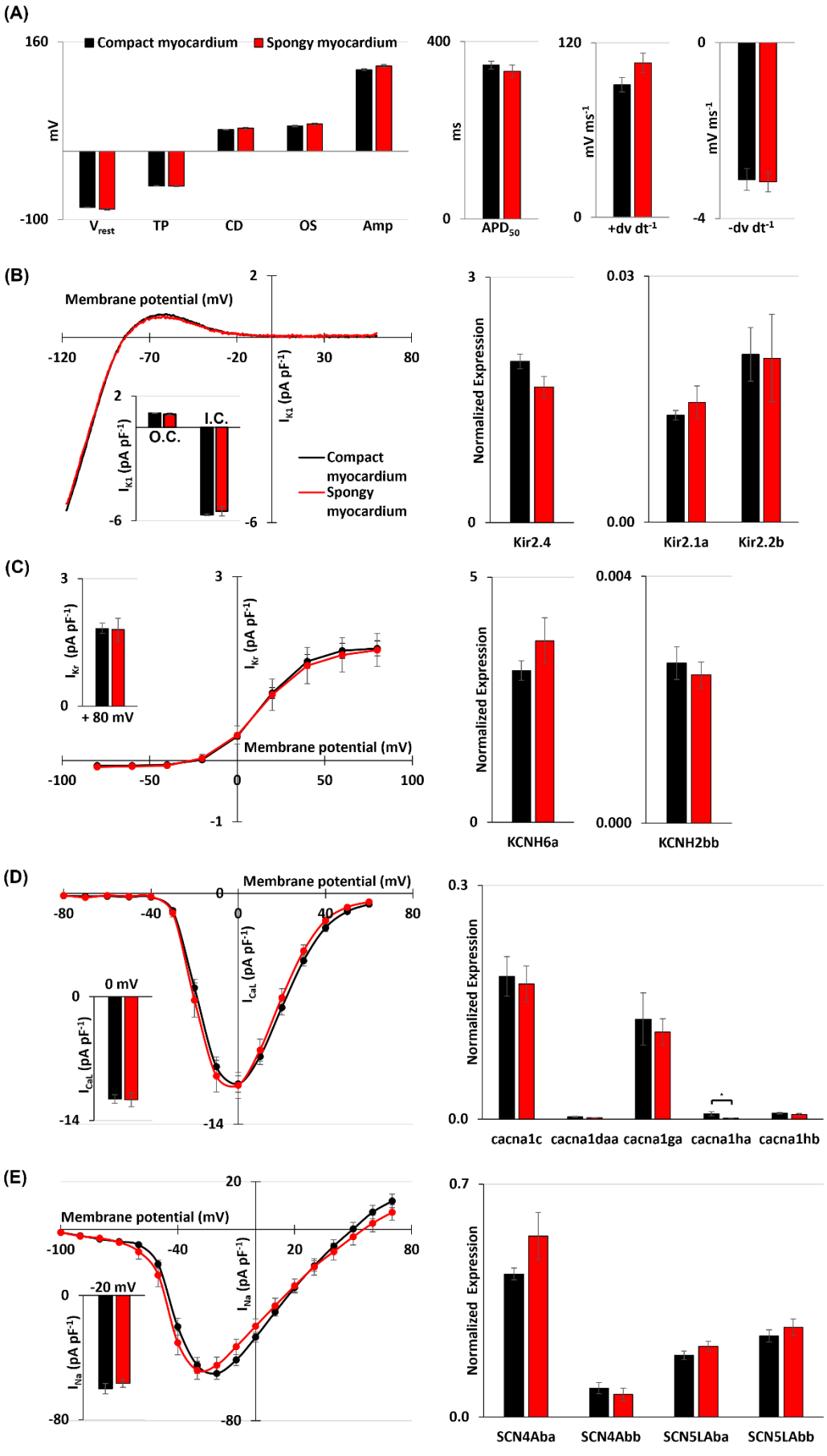
(A)
Compact myocardium
Spongy myocardium
mV
160
-100
V_{rest}
TP
CD
OS
Amp
ms
400
0
APD_{50}
mV ms^{-1}
120
0
+dv dt^{-1}
0
-4
-dv dt^{-1}
(B)
Membrane potential (mV)
-120
-70
-20
30
80
2
-6
I_{K1} (pA pF^{-1})
O.C.
I.C.
Compact myocardium
Spongy myocardium
Normalized Expression
3
0
Kir2.4
0.03
0.00
Kir2.1a
Kir2.2b
(C)
I_{Kr} (pA pF^{-1})
+ 80 mV
Membrane potential (mV)
-100
-50
50
100
-1
5
KCNH6a
0.004
0.000
KCNH2bb
(D)
Membrane potential (mV)
-80
-40
40
80
0 mV
I_{CaL} (pA pF^{-1})
-14
0.3
0.0
cacna1c
cacna1daa
cacna1ga
cacna1ha
cacna1hb
(E)
Membrane potential (mV)
-100
-40
20
80
-20 mV
I_{Na} (pA pF^{-1})
-80
0.7
SCN4Aba
SCN4Abb
SCN5LAba
SCN5LAbb

Fig. S1. Comparison of action potential (AP) parameters, sarcolemmal ion currents, and ion channel expression between compact (pooled data from apex, middle and basal regions) and spongy myocardium of rainbow trout ventricle. (**A**) Ventricular APs parameters: resting membrane potential (V_{rest}), threshold potential for AP initiation (TP), critical depolarization (CD), AP overshoot (OS), AP amplitude (Amp), AP duration at 50% level of repolarization (APD_{50}), maximum rate of depolarization (+dV dt^{-1}), and repolarization (-dV dt^{-1}). (**B-C**) Inward (I_{K1}) and delayed rectifier (I_{Kr}) K^+ currents (left), and transcripts of Kir2 (I_{K1}), KCNH2bb and KCNH6a (I_{Kr}) channels (right). The insets show peak densities of inward (I.C.) and outward (O.C) of I_{K1} (**B**), and peak tail current densities of I_{Kr} at +80 mV (**C**). (**D-E**) Ca^{2+} (I_{CaL}) and Na^+ (I_{Na}) currents (left), and transcripts of Ca^{2+} and Na^+ channels (right). The insets show the peak current densities of I_{CaL} at 0 mV (**D**), and I_{Na} at -20 mV (**E**). An asterisk (*) indicates statistically significant differences ($p < 0.05$; *t*-test) between mean values.

Dataset 1.

Click here to download Dataset 1